Journal of Extracellular Vesicles

COACTION PUBLISHING

ORIGINAL RESEARCH ARTICLE

Comparative analysis of discrete exosome fractions obtained by differential centrifugation

Dennis K. Jeppesen[1], Michael L. Hvam[2,3], Bjarke Primdahl-Bengtson[1], Anders T. Boysen[2,3], Bradley Whitehead[2,3], Lars Dyrskjøt[1], Torben F. Ørntoft[1], Kenneth A. Howard[2,3] and Marie S. Ostenfeld[1]*

[1]Department of Molecular Medicine, Aarhus University Hospital, Aarhus, Denmark; [2]The Interdisciplinary Nanoscience Center (iNANO), University of Aarhus, Aarhus, Denmark; [3]Department of Molecular Biology and Genetics, University of Aarhus, Aarhus, Denmark

Background: Cells release a mixture of extracellular vesicles, amongst these exosomes, that differ in size, density and composition. The standard isolation method for exosomes is centrifugation of fluid samples, typically at 100,000 × *g* or above. Knowledge of the effect of discrete ultracentrifugation speeds on the purification from different cell types, however, is limited.

Methods: We examined the effect of applying differential centrifugation g-forces ranging from 33,000 × *g* to 200,000 × *g* on exosome yield and purity, using 2 unrelated human cell lines, embryonic kidney HEK293 cells and bladder carcinoma FL3 cells. The fractions were evaluated by nanoparticle tracking analysis (NTA), total protein quantification and immunoblotting for CD81, TSG101, syntenin, VDAC1 and calreticulin.

Results: NTA revealed the lowest background particle count in Dulbecco's Modified Eagle's Medium media devoid of phenol red and cleared by 200,000 × *g* overnight centrifugation. The centrifugation tube fill level impacted the sedimentation efficacy. Comparative analysis by NTA, protein quantification, and detection of exosomal and contamination markers identified differences in vesicle size, concentration and composition of the obtained fractions. In addition, HEK293 and FL3 vesicles displayed marked differences in sedimentation characteristics. Exosomes were pelleted already at 33,000 × *g*, a g-force which also removed most contaminating microsomes. Optimal vesicle-to-protein yield was obtained at 67,000 × *g* for HEK293 cells but 100,000 × *g* for FL3 cells. Relative expression of exosomal markers (TSG101, CD81, syntenin) suggested presence of exosome subpopulations with variable sedimentation characteristics.

Conclusion: Specific g-force/*k* factor usage during differential centrifugation greatly influences the purity and yield of exosomes. The vesicle sedimentation profile differed between the 2 cell lines.

Keywords: *extracellular vesicles*; *exosomes*; *microvesicles*; *nanoparticle tracking analysis*; *differential centrifugation*; k *factor*

Responsible Editor: Elena Aikawa, Harvard Medical School, United States.

*Correspondence to: Marie S. Ostenfeld, Department of Molecular Medicine, Aarhus University Hospital, Brendstrupgaardsvej 100, DK-8200 Aarhus, Denmark, Email: marie.stampe@clin.au.dk

To access the supplementary material to this article, please see Supplementary files under Article Tools online.

Received: 23 May 2014; Revised: 20 August 2014; Accepted: 26 September 2014; Published: 6 November 2014

Membrane vesicles of heterogeneous size and composition are released from most, if not all, types of cells studied so far (1,2) and are found in the extracellular space and human biofluids (3,4). The vesicles are known to be important agents of intracellular communication, and as we recently demonstrated for FL3 exosomes may also function as route of cellular disposal (5,6). The extracellular space will contain a mixture of vesicles that display specific markers that can uniquely identify their subcellular origin (7). The macromolecule content of the vesicles can be transferred to a recipient cell by uptake, with functional consequences (8). The nomenclature for vesicle research is still being developed (9). In this report, we will use the term "extracellular vesicle" (EV) to encompass all membrane vesicles released from cells while the terms "exosomes," "microvesicles," "apoptotic bodies" and "microsomes" are used for specific populations of EVs. Exosomes, one of the most studied of the EVs, are small membrane vesicles (40–100 nm) of endocytic origin that are released by

fusion of intracellular multivesicular bodies with the cell membrane. Using centrifugation, exosomes are typically isolated by sedimentation at 100,000–200,000 $\times g$ (2,10). Another commonly described type of EV is microvesicles, which have been proposed to have a typical diameter of 100–1,000 nm and released by budding of the cell plasma membrane (2,11). Microvesicles are typically reported to be isolated by centrifugation at 10,000–20,000 $\times g$ (9). Cells undergoing apoptosis show irregular buds of the plasma membrane known as blebs, and the cell will eventually break apart forming membrane vesicles called apoptotic bodies or blebs. Apoptotic bodies are 50–5,000 nm in size and have typically been isolated at a g-force of $\sim$2,000 $\times g$. Microsomes are small 80–120 nm vesicles formed from fragments of endoplasmic reticulum (ER) membrane (12,13).

The nano-scale size of exosomes presents a challenge, not only for size determination but also for accurate quantification. Recently, nanoparticle tracking analysis (NTA), a technique for sizing and counting vesicles and particles in solution, based on Brownian motion, has gained widespread application in the study of EVs (14,15). This NTA method has been widely utilized for determination of both the size as well as the concentration of EVs (14,16), and we used this technique in this work to analyse the EVs present in supernatants and resuspensions of sedimented vesicles after ultracentrifugation.

The most widely applied, and basic, method for separating exosomes from cells, apoptotic bodies, and microvesicles is differential centrifugation (10,17). The sedimentation of vesicles depends on their size, density, and shape as well as the viscosity of the sample solution. The differential centrifugation scheme utilizes these sedimentation characteristics to first remove cells and non-exosomal EVs before the presumed exosomes are pelleted by a single high g-force step. But this centrifugation approach to exosome isolation will co-purify other non-EV components present in culture media or biological fluid. Therefore, the crude exosome preparation generated by centrifugation is commonly used as the input for more sophisticated centrifugation procedures such as sucrose cushions (18), or gradients of sucrose (19,20) or iodixanol (21,22) that attempts to further separate vesicles and particles based on floatation densities. However, the use of cushions and gradients, adds to the time required for purification and results in loss of sample material. It is also presently unclear if the biological and functional characteristics of exosomes are altered by floatation in gradients. In addition, care must be taken as high-density lipoproteins may be co-purified with EVs in density gradients (23).

As the differential centrifugation method is the first-line technique for routine preparations of exosomes, we examined the effect of using different centrifugal g-forces on vesicle size and concentration, protein yield, and exosomal markers. For this, we employed 2 different, but complementary, schemes of centrifugation. First, a parallel approach where the input material was subjected to a single 33,000 $\times g$ (33k) to 200,000 $\times g$ (200k) ultracentrifugation step. Next, a serial depletion approach where the input material was repeatedly depleted by a series of increasing centrifugal force steps from 33k to 200k. This allowed us to, first, determine the most efficient sedimentation speed in terms of the highest ratio of vesicles to pelleted protein and content of exosomal markers and, second, to evaluate if the material being deposited at lower speeds differed from the material pelleted at higher speeds. Furthermore, 2 cell types, embryonic kidney HEK293 cells and bladder carcinoma FL3 cells, were used to study possible differences attributed to cell type origin.

Materials and methods

Cell lines and culture conditions

Human urinary bladder transitional cell carcinoma FL3 cells were maintained in Dulbecco's Modified Eagle's Medium (DMEM), with or without phenol red, 10% fetal bovine serum and 100 μg/ml penicillin–streptomycin as well as in advanced DMEM (Gibco Invitrogen, Carlsbad, CA, USA). Cell-line authentication was performed using short tandem repeat (STR) profiling (Cell ID System, Promega, Madison, WI, USA). Human embryonic kidney 293 cells (HEK293) were cultured in a similar manner. Both cell lines were regularly tested negative for mycoplasma by nested polymerase chain reaction (PCR) analysis. Cells were seeded at 25×10^6 cells in a 15 ml volume into the lower cell chamber of CELLine Adhere 1000 bioreactors (INTEGRA Biosciences AG, Zizers, Switzerland) and maintained at high culture density at 37°C in a 5% CO_2 humidified incubator, essentially as previously described (24). The chamber occupied by the cells contained medium with serum depleted for contaminating EVs by overnight ultracentrifugation at 200,000 $\times g$. Cell-conditioned media (CCM) was harvested from the bioreactor every 96 hours, and the viability of cell growing in the bioreactors periodically assessed.

Centrifugation and ultracentrifugation

Cell culture medium (DMEM) was added 20% FCS, centrifuged at 100,000 $\times g$ or 200,000 $\times g$ for 16 hours after which it was sterile-filtered and diluted to a final concentration of 10% FCS. The different media types were added to cells to examine possible negative impact on cell viability using MTT assays.

For NTA and protein analysis, CCM was immediately (after harvest from cultured cells) subjected to a series of centrifugation steps in a 5804 R centrifuge at 4°C using a F34-6-38 fixed angle rotor (Eppendorf), first at 400 $\times g$ for 10 min then at 2,000 $\times g$ for 20 min and finally at 15,000 $\times g$

Citation: Journal of Extracellular Vesicles 2014, **3**: 25011 - http://dx.doi.org/10.3402/jev.v3.25011

for 30 min. At each step, the supernatant was transferred to new tubes and the pellets immediately resuspended in either PBS or rinsed with PBS and then resuspended in lysis buffer (20 mM Tris-HCl (pH 7.5), 150 mM NaCl, 1 mM Na2EDTA, 1 mM EGTA, 1% Triton X, 2.5 mM sodium pyrophosphate, 1 mM beta-glycerophosphate, 1 mM Na3VO4, 1 μg/ml leupeptin), and the supernatants and resuspended pellet material immediately taken for NTA measurements. These pre-cleared supernatants were stored at −80°C until further use (for parallel and serial ultracentrifugation followed by NTA and protein analysis). All ultracentrifugation steps were performed in an Optima XPN80 ultracentrifuge using a Type 70 Ti fixed angle rotor (Beckman Coulter, FL, USA) at 4°C for 90 min. Centrifugation of material from FL3 and HEK293 cells was performed simultaneously. After ultracentrifugation, sample pellets were immediately resuspended in either PBS or lysis buffer, and the supernatants and resuspended pellet material immediately taken for NTA measurements. An overview of the centrifugation steps, including relative centrifugal force (RCF), revolutions per minute (RPM) and the adjusted k factors (k_{adj}), is presented in Table 1. RPM was calculated from RCF according to Equation 1 while adjusted k factors were calculated according to Equation 3 (Supplementary File 1).

MTT viability assay

FL3 and HEK293 cells were seeded at 20,000 and 33,000 cells/cm^2 into 96-well plates in DMEM with 10% FBS and 100 μg/ml penicillin–streptomycin. The following day, media was removed from the 20–30% confluent cells, the cells washed with PBS and new media of various compositions was added. After 48 hours, cell density was assessed by the 3-(4,5-dimethylthiazole-2-y)-2,5-diphenyltetrasodiumbromide (MTT, Sigma-Aldrich, St Louis, MO, USA) reduction assay, essentially as described previously (25).

Nanoparticle tracking analysis

Particles present in samples were analysed by nanoparticle tracking, using the NanoSight LM10 system (NanoSight Ltd, Amesbury, UK), configured with a 405 nm laser and a high-sensitivity sCMOS camera (OrcaFlash2.8, Hamamatsu C11440, NanoSight Ltd). Videos were collected and analysed using the NTA software (version 2.3, build 0025), with the minimal expected particle size, minimum track length and blur setting, all set to automatic. Ambient temperature was recorded manually and did not exceed 25°C. Each sample was diluted in particle-free PBS and had a final volume of 0.4 ml. Samples were analysed within 15 min of the initial dilution with a delay of 10 seconds between sample introduction and the start of the measurement (16). Approximately 20–40 particles were in the field of view and the typical concentration was approximately 2×10^8–10×10^8 particles/ml for each measurement to keep within the linear range (14). For each sample, multiple videos of 60 seconds duration were recorded generating replicate histograms that were averaged. The typical number of completed and tracked events per measurements typically exceeded 2000, and 5 measurements taken per sample.

Cellular and vesicle protein extraction and protein quantification

To extract cellular proteins, FL3 and HEK293, cells were harvested, washed twice with ice-cold PBS, and solubilized in lysis buffer (20 mM Tris-HCl (pH 7.5), 150 mM NaCl, 1 mM Na2EDTA, 1 mM EGTA, 1% Triton X, 2.5 mM sodium pyrophosphate, 1 mM beta-glycerophosphate, 1 mM Na3VO4, 1 μg/ml leupeptin) to which complete Mini protease inhibitor cocktail, PhosSTOP phosphatase inhibitor cocktail (both from Roche) and 2.0 mM Pefabloc (Sigma-Aldrich, St Louis, MO, USA) were added immediately before use, on ice for 30 min. Cell lysates were centrifuged at 11,000 × g at 4°C to remove cellular debris. The pellets obtained after

Table 1. Relative centrifugal forces, speed, adjusted clearing factor and run times

Abbreviation	Average RCF	Speed (RPM)	Rotor type	Adjusted k factor (k_{adj})	Run time (min)
0.4k	400 × g	1,764	F34-6-38 fixed angle	80853.2[a]	10
2k	2,000 × g	3,944	F34-6-38 fixed angle	16174.1[a]	20
15k	15,000 × g	10,801	F34-6-38 fixed angle	2156.6[a]	30
33k	33,000 × g	21,196	Type 70 Ti fixed angle	479.9[b]	90
67k	67,000 × g	30,202	Type 70 Ti fixed angle	236.4[b]	90
100k	100,000 × g	36,897	Type 70 Ti fixed angle	158.4[b]	90
133k	133,000 × g	42,552	Type 70 Ti fixed angle	119.1[b]	90
167k	167,000 × g	47,682	Type 70 Ti fixed angle	94.8[b]	90
200k	200,000 × g	52,181	Type 70 Ti fixed angle	79.2[b]	90

[a]Calculated for the F34-6-38 fixed angle rotor (Eppendorf, k factor of 2,079 at 11,000 RPM using 50 ml tube inserts) with tubes filled to nominal capacity.
[b]Calculated for the Type 70 Ti fixed angle rotor (Beckman Coulter, k factor of 44 at 70,000 RPM) with tubes filled to nominal capacity.

400 × *g*, 2,000 × *g* and 15,000 × *g* centrifugation were likewise, after washing and repelleting, solubilized in lysis buffer. Protein content of the cell and vesicle lysates were quantified by Bradford microassays (Bio-Rad, Hercules, CA, USA) with comparison against a BSA standard curve. Values were extrapolated from this fitted curve, with $r^2 > 0.99$ for all included measurements.

One-dimensional electrophoresis and immunoblotting

Samples were suspended in sample buffer (2% SDS, 10% glycerol, 50 mM Tris-HCl pH 6.8, bromophenol blue) and subjected to denaturing electrophoresis using precast Novex 4–12% or 12% Bis–Tris NuPAGE gels (Invitrogen, Carlsbad, CA, USA) in MOPS running buffer at constant 150 V for 75 min. Proteins were electrotransferred onto Immobilon PVDF membranes (Millipore, MA, USA), and the membranes blocked with 5% (w/v) skimmed milk powder in PBS with 0.1% (v/v) Tween-20 (PBST) for 1 hour at RT. Membranes were probed with the following primary antibodies: CD81 (Santa Cruz), syntenin (Abcam), calreticulin (BioVision, Mountain View, CA, USA), VDAC1 (Abcam) and TSG101 (Santa Cruz) followed by incubation with appropriate HRP-conjugated secondary antibodies (DAKO A/S, Glostrup, Denmark) in blocking buffer. The immunoblots were visualized using ECL Prime agents (Amersham Biosciences, Buckinghamshire, UK) and imaged on the ChemiDoc (Bio-Rad, Hercules, CA, USA). Membranes were exposed for short durations to prevent saturation of blots allowing the relative protein expression levels to be determined by densitometry using ImageJ 1.46r software (National Institutes of Health, Bethesda, Maryland, USA) following the protocol outlined in the ImageJ instruction manual. Longer exposures of the membranes were also performed for enhanced detection of low expression levels.

Statistics

Statistical analyses were performed using the SPSS Statistical Analysis System (version 21.0; SPSS Inc., Chicago, IL). Normal distribution of data sets was assessed by Shapiro–Wilks tests and visual inspection of Q–Q plots. Equality of variance was tested by Levene's test where appropriate. Sphericity was tested by Mauchly's test where appropriate. All data are presented as mean ± s.e.m., unless otherwise stated. To assess differences between 2 groups, Student's t-test (paired or unpaired, 2-tailed) or the Wilcoxon signed rank test was used, as applicable. When 3 or more groups were compared, either 1-way repeated measures ANOVA or the Friedman test was used. Pairwise comparisons of groups were corrected for multiple comparisons by the Holm–Bonferroni procedure. Differences were considered to be significant for values of $p < 0.05$.

Results

To investigate the influence of exact differential centrifugation g-force on the yield and purity of exosomes, we analysed 2 unrelated human cell lines, FL3, a urinary bladder transitional cell carcinoma cell line (26), and HEK293. As mycoplasma bacteria are ~100–125 nm in size and a common obstacle in cell cultivation, mycoplasma infections present a potential problem for accurate exosome measurements (27,28). The cells used in the study were, therefore, importantly tested and found to be negative for mycoplasma. All ultracentrifugation steps were performed for 90 min as examination suggested no increase in pelleted material from 90 to 120 min (Supplementary Fig. 1).

Measurements of vesicle size by NTA are commonly performed on PBS-resuspended particle pellets (14,16). We performed an initial NTA analysis on FL3 CCM first pre-cleared by 400 to 15,000 × *g* (0.4–15k) centrifugation steps and then subjected to a single ultracentrifugation step at 100,000 × *g* (100k). The size of particles increased when comparing the measurement in pre-cleared CMM versus the pellet obtained by 100k (mode size: 82 nm → 106 nm, mean size: 120.6 nm → 144.4 nm) (Fig. 1a). This size difference was also observed when comparing the input (15k) supernatant with the sum of output (100k pellet and supernatant) (Fig. 1b). The size discrepancy may indicate that vesicle aggregation occurs during pelleting. Subsequent vesicle quantifications by NTA were, therefore, primarily performed on supernatants.

Cell medium used for exosome isolation is commonly depleted for bovine exosomes by overnight ultracentrifugation. We next examined various media types to identify the medium generating the least amount of background particles amounts as measured by NTA. There was a significant difference ($p < 0.00001$) between the quantities of particles present in the different media types and a substantial number of particles even in serum-free Advanced DMEM medium (Fig. 2a). When comparing DMEM medium with serum, the lowest number of particles was found in phenol red-free medium depleted for bovine exosomes by 16 hours overnight ultracentrifugation at 200,000 × *g* (200k). The mode and mean size of the particles present in the different types of media ranged from 68–89 to 95–110 nm, respectively, thus placing them in the size range of exosomes (Fig. 2b).

To assess whether sedimentation of serum components reduced the viability of FL3 and HEK293 cells, MTT viability assays were performed using the different media types. The viability did not differ appreciably between the different types of DMEM with the exception of Advanced DMEM with phenol red which markedly lowered the viability for FL3 cells (Fig. 2c).

We next tested if traces of media impacted the measurement of particle size. No significant change in mode size of 100 nm control nano-beads was observed in

Citation: Journal of Extracellular Vesicles 2014, **3**: 25011 - http://dx.doi.org/10.3402/jev.v3.25011

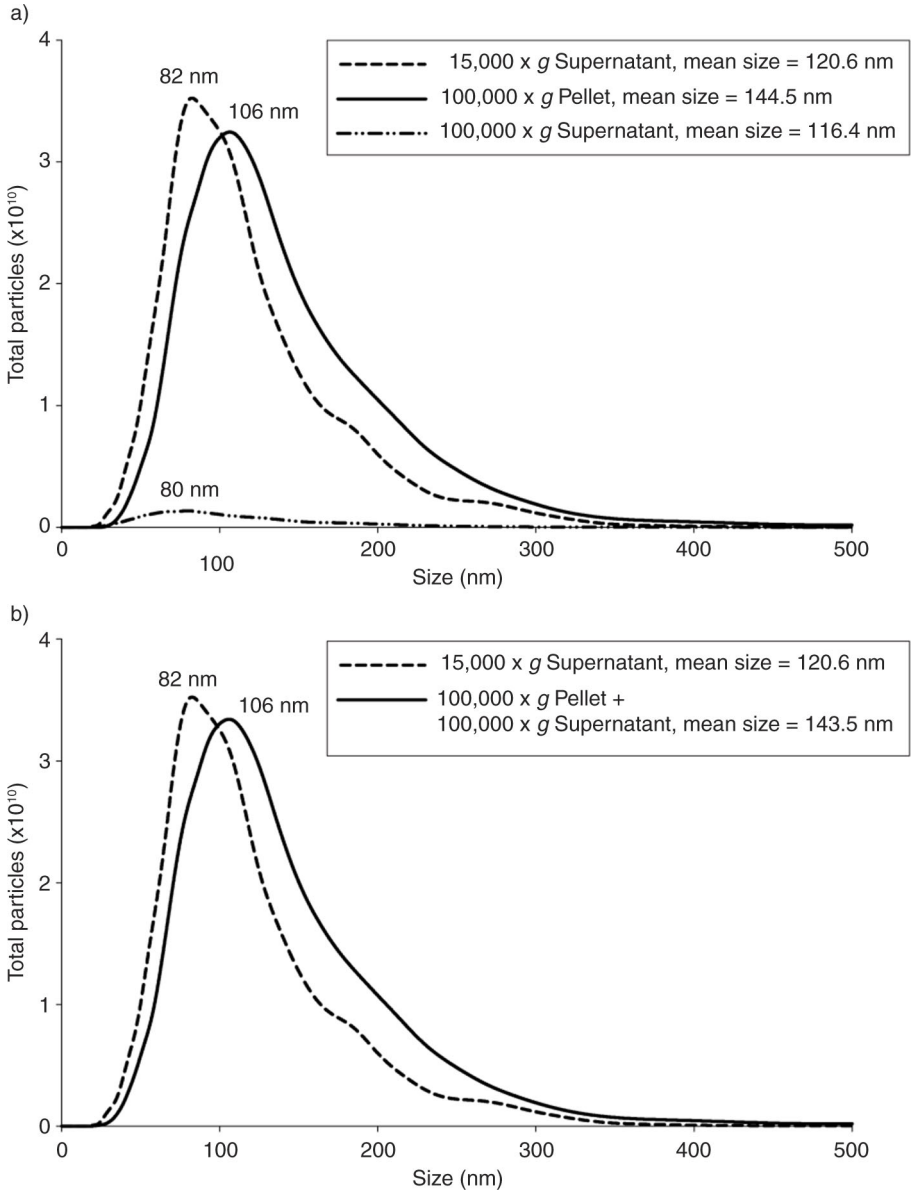

Fig. 1. Size profile of comparison of FL3 particles in supernatants and pellet. FL3 cells were cultured in DMEM without phenol red but with serum depleted for bovine exosomes by 200,000 × *g* ultracentrifugation for 16 hours. (a) FL3 cell-conditioned media (CCM) was harvested and first pre-cleared by 400–15,000 × *g* centrifugation steps and then subjected to a single ultracentrifugation step at 100,000 × *g*. Supernatants and pellet were diluted in particle-free PBS and the particles present measured using the NanoSight NTA system. Average plots of the overall size distribution of particles are based on 5 repeat measurements. (b) Plots of size distribution of the input 15,000 × *g* supernatant and the sum of the 100,000 × *g* pellet and supernatant output.

PBS versus 1:10 PBS-diluted media suspensions (Supplementary Fig. 2a). We examined mixed suspension of 100 and 200 nm control beads. Two clearly separate peaks representing the 2 types of control beads was observed, demonstrating that NTA could accurately detect and distinguish particles of different sizes present in the same solution (Supplementary Fig. 2b). Finally, we consistently observed that inclusion of phenol red in the media introduced haziness to the videos captured for NTA (observations). Altogether, our data pointed towards the usage of 200k-depleted medium without phenol red for optimal NTA measurements of particles and that this did not hamper cell viability. Importantly, measurements on CCM supernatant showed expected control particle size and were more suitable for quantitative analysis than pellet analysis.

We finally tested the effect of partial filling of centrifugation tubes on the sedimentation characteristics. Filling tubes to less than nominal capacity should theoretically lower the effective *k* factor because of the

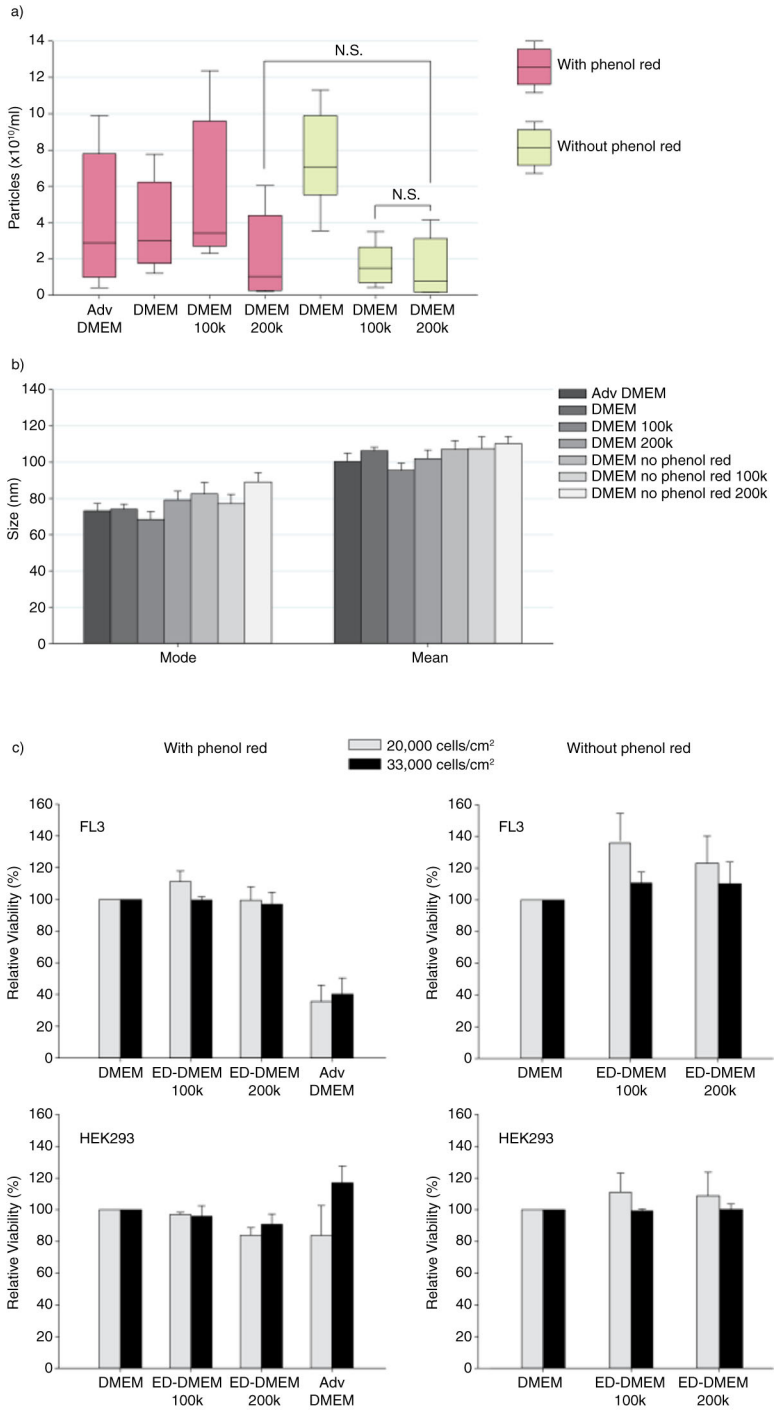

Fig. 2. Analysis of particles present in different media types and effect on viability of cell growth. (a) Media samples of DMEM with either 8% foetal bovine serum or 8% serum depleted for bovine exosomes (100k and 200k, serum-containing medium cleared of bovine exosomes by 16 hours ultracentrifugation at 100,000 × *g* or 200,000 × *g* of 20% serum solutions, respectively) with and without addition of phenol red, as well as Advanced DMEM, were analysed using NTA. All media types were centrifuged at 15,000 × *g* before analysis. Measurements of particle concentration were made in triplicate for each of the samples. Data are expressed as mean ± s.e.m. (n = 12 per group generated from 3 independent experiments). P-value for difference between groups was determined by the Friedman test while p-values between pairs of groups were determined by Wilcoxon signed rank tests and corrected for multiple comparisons by the Holm–Bonferroni procedure. N.S., not significant. (b) The mode and mean size of particle in media measured by NTA. (c) The viability of FL3 cells and HEK293 cells grown in various types of DMEM media with (*left*) or without (*right*) phenol red at seeding densities of 20,000 or 33,000 cells/cm^2 were examined by MTT assays. Data are expressed as mean ± s.e.m. (for FL3 n = 3 and for HEK293 n = 4 per group generated from 3 independent experiments).

Citation: Journal of Extracellular Vesicles 2014, **3**: 25011 - http://dx.doi.org/10.3402/jev.v3.25011

shortened average path length a particle has to travel for sedimentation, and therefore require shorter centrifugation run times (Supplementary File 1). Consistent with this, we observed significantly more sedimentation of material when using partially filled tubes (Supplementary Fig. 3a). This could be adjusted for when reducing the run time appropriately according to the difference in effective *k* factor (Supplementary Fig. 3b).

Parallel ultracentrifugation–comparative analysis by NTA, protein quantification and immunoblotting

To examine the optimal centrifugal force for isolation of exosomes, we employed a parallel ultracentrifugation approach (Fig. 3a). Pre-cleared CCM was split into equal volumes that were then subjected to a single ultracentrifugation step at a centrifugal force ranging from 33k to 200k. The size profiles of the particles in pre-cleared 15k CCM supernatants (input) revealed that the peak (mode) size of particles was 98 and 140 nm for FL3 and HEK293 CCM, respectively (Fig. 4a). The size profile of particles remaining in the supernatant (output) after the ultracentrifugation step (Fig. 4a, supernatant) did not markedly differ between FL3 and HEK293 (mode size ~100 nm).

The mode size of FL3 EVs differed substantially when measured in suspension versus measurement of resuspended pellets (Fig. 1). We, therefore, compared the size profile of HEK293 EVs in pre-cleared CCM suspension, and after resuspension of sedimented pellets. The measured mode size of particles after pelleting and resuspension was 147, 153 and 158 nm for g-forces of 33k, 67k and 100k, respectively, and thus 7–18 nm higher than the measured 140 nm mode size of particles in pre-cleared 15k CCM (Fig. 4a). After pelleting at the higher g-forces of 167k and 200k, 2 clearly separate peaks representing population of particles of 68, 146 and 149 nm, respectively, became noticeable.

The pattern of particles sedimented from supernatants with increasing g-force differed between FL3 and HEK293 (Fig. 4b). Only a small fraction of FL3 particles were pelleted at 33k and 67k, whereas a predominant fraction of HEK293 particles were pelleted here. In addition, a substantially larger fraction of FL3 particles were resistant to sedimentation at speeds over 100k, which was not the case for HEK293 particles. The depletion of particles from the supernatants with increasing speed was reflected in the increase of particles found in sedimented pellets (Supplementary Fig. 4). The fraction of 1–100 nm

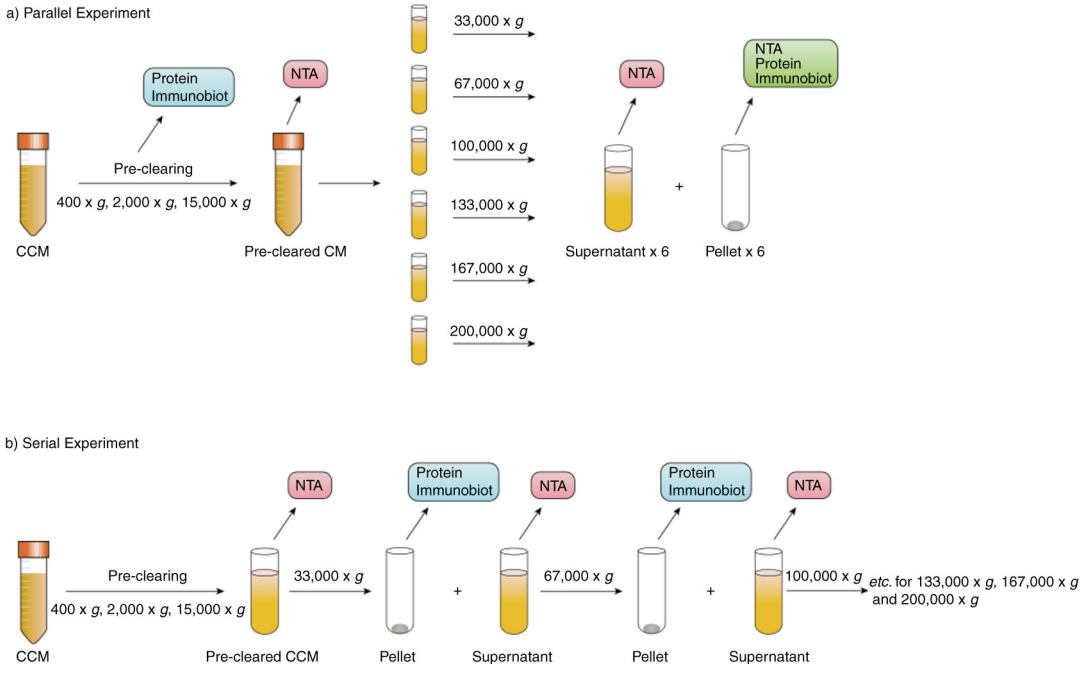

Fig. 3. Differential ultracentrifugation experimental schemes. (a) Parallel differential ultracentrifugation. Harvested FL3 and HEK293 CCM was subjected first to a series of pre-clearing centrifugation steps of increasing relative centrifugal force (RCF) (0.4–15k, Table 1) with the resulting supernatant in each step being used as the input for next step while the pellets were subjected to lysis before protein determination and immunoblot analysis. The pre-cleared CCM was split into aliquots of 6 equal volumes and each aliquot subjected to ultracentrifugation at a RCF ranging from 33k to 200k (Table 1). Samples of supernatant were taken for NTA measurements while the pellets were either resuspended in particle free-PBS or subjected to lysis before protein determination and immunoblot analysis. (b) Serial differential ultracentrifugation. Pre-cleared CCM was subjected to a series of ultracentrifugation steps of increasing RCF from 33k to 200k (Table 1) with the resulting supernatant in each step being used as the input for next step. Samples of supernatant were taken for NTA measurements while the pellets were subjected to lysis before protein determination and immunoblot analysis.

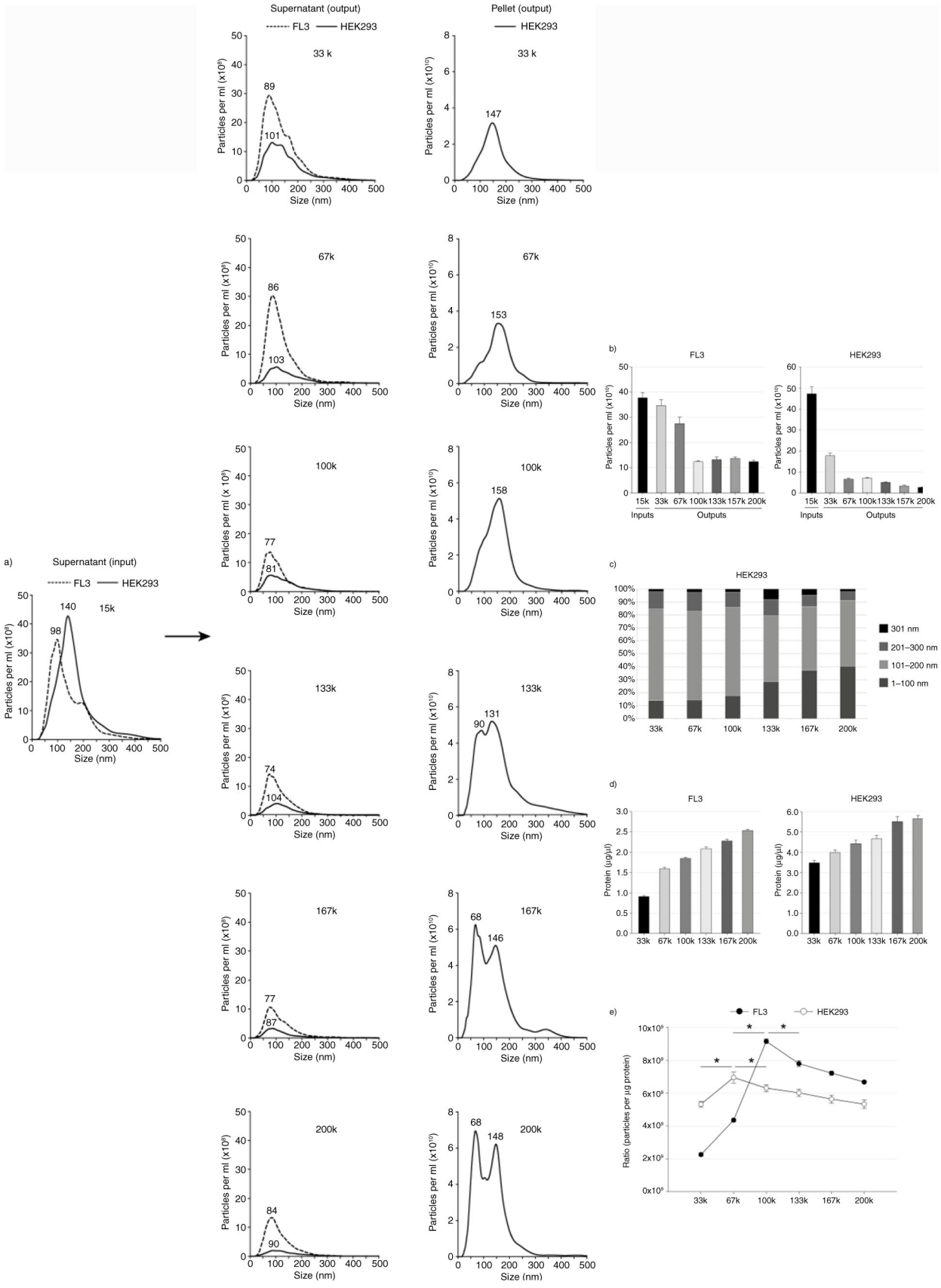

Fig. 4. Continued

Citation: Journal of Extracellular Vesicles 2014, **3**: 25011 - http://dx.doi.org/10.3402/jev.v3.25011

particles in pellets of HEK293 was enriched with increasing speed (Fig. 4c). For both FL3 and HEK293, there was a clear increase in sedimentation of protein with rising g-force but with significantly more protein sedimented at a force over 33k for FL3 (Fig. 4d, left) while for HEK293 the difference between 33k and higher speeds was less pronounced (Fig. 4d, right). HEK293 cells were generally observed to release a greater abundance of vesicles than FL3 cells when particles in the supernatant and the protein content of pelleted material were measured (Fig. 4b and d). Previously, the ratio of particles-to-protein has been suggested as a measure for the purity of vesicle samples (29). We calculated the number of particles sedimented at the different parallel ultracentrifugation speeds and plotted the ratio of particles to protein (Fig. 4e). The highest ratio was achieved at 67k for HEK293 and 100k for FL3. These data indicate that the sedimentation efficiency of particles from HEK293 and FL3 cells differed significantly.

Immunoblotting was performed on the pellets of EVs generated by the parallel ultracentrifugation experiments (Fig. 5). TSG101 is a commonly accepted cytosolic ESCRT protein marker of exosomes involved in formation of multivesicular bodies (30). For both FL3 and HEK293 exosomes, the highest TSG101 signal was found in pellets after 67k. At 33k and the higher speeds of 167k and 200k the signal was markedly lower indicating that exosomes contributed less to the total pelleted material at these speeds. For both cell lines TSG101 was highly enriched in exosome samples compared to the parental cell lines (pelleted at 0.4k), apoptotic bodies (pelleted at 2k) and microvesicles (pelleted at 15k). Syntenin, another exosomal marker, is a key regulator of exosome biogenesis (21) and we observed it to be most abundantly present in the 100k pellet for FL3, and in the 67k pellet for HEK293. To assess the presence of mitochondrial contamination we analysed pelleted material for the protein VDAC1, a previously used contamination marker (31,32). For both FL3 and HEK293, VDAC1 could be detected in cell lysates as well as apoptotic bodies but not in microvesicles, and not in any of the exosome fractions. When eukaryote cells undergo apoptosis, fragments of the ER membrane can form small 80–120 nm vesicle-like entities termed microsomes that can be pelleted by ultracentrifugation, commonly at speeds in the range of 100k (12,13). The level of the ER marker protein, calreticulin, was markedly reduced in exosome samples compared to preparations of cells, apoptotic bodies and microvesicles. These data suggest, based on exosomal marker proteins, that the most optimal ultracentrifugation speed for purification is 100k for FL3 and 67k for HEK293.

Serial ultracentrifugation–comparative analysis by NTA, protein quantification and immunoblotting

Next, we examined if the material being deposited at the lower g-forces differed from the material pelleted at higher speeds by using a serial scheme of increasing sedimentation velocities (Fig. 3b). Pre-cleared CCM was subjected to 6 rounds of ultracentrifugation at 33–200k with the supernatant generated after each round used as the input for the next in order to follow the depletion of particles from the sample. The mode size of particles present in pre-cleared CCM from FL3 and HEK293 cells was 102 and 144 nm, respectively (Fig. 6a). The concentration of particles present in CCM supernatant declined with each serial step of ultracentrifugation, but to a greater extent for HEK293 than FL3 (Fig. 6b). Almost 90% of HEK293 particles were cleared by a g-force of less than the 100k commonly used for isolation of exosomes. Regarding

Fig. 4. Parallel differential ultracentrifugation. (a) Pre-cleared FL3 and HEK293 CCM supernatants (15k), and supernatants and pellets generated by ultracentrifugation steps (33–200k) were diluted in particle-free PBS and the particles present measured using the NanoSight NTA system. Average plots of the overall size distribution of particles are based on 5 repeat measurements and represent the profile of particles present in the supernatant after the indicated ultracentrifugation step (supernatant, *left*) or in the resulting sedimentation pellet (Pellet, *right*). (b) Quantification by NTA of particles present in supernatants generated from pre-cleared CCM harvested from FL3 (*left*) and HEK293 (*right*) cells, and subjected to parallel ultracentrifugation steps. Data are expressed as mean ± s.e.m. (n = 5 per group), p-value for overall difference between groups was determined by repeated measures ANOVA (Greenhouse-Geisser corrected) and p-values between pairs of groups were determined by Student's paired t-tests with correction for multiple comparisons by the Holm–Bonferroni procedure. *$p < 0.05$; **$p < 0.0001$; N.S., not significant. (c) Population of particles of defined size ranges after depletion of HEK293 CCM by ultracentrifugation. The size of particles was measured by NTA in sedimentation pellets after ultracentrifugation steps of relative centrifugal force (RCF) from 33k to 200k. The fraction of the total population in the size ranges 1–100nm, 101–200 nm, 201–300 nm and 301+ nm was plotted. (d) Quantification of protein in sedimentation pellets generated by 33k to 200k parallel ultracentrifugation steps and solubilization in equal volumes of lysis buffer. Data are expressed as mean ± s.e.m. (n = 12 per group), p-value for overall difference between groups was determined by repeated measures ANOVA (Greenhouse–Geisser corrected) and p-values between pairs of groups were determined by Student's paired t-tests with correction for multiple comparisons by the Holm–Bonferroni procedure. *$p < 0.05$; N.S., not significant. (e) The number of pelleted particles was calculated from the input and output supernatants, and the ratio of particles per μg of protein pelleted after parallel ultracentrifugation (33–200k) was plotted. Data are expressed as mean ± s.e.m. (n = 6 per group), p-value for overall difference between groups was determined by repeated measures ANOVA (Greenhouse–Geisser corrected) and p-values between pairs of groups were determined by Student's paired t-tests with correction for multiple comparisons by the Holm–Bonferroni procedure. *$p < 0.05$. Reported statistical significance is relative to the maxima (67k for HEK293 and 100k for FL3).

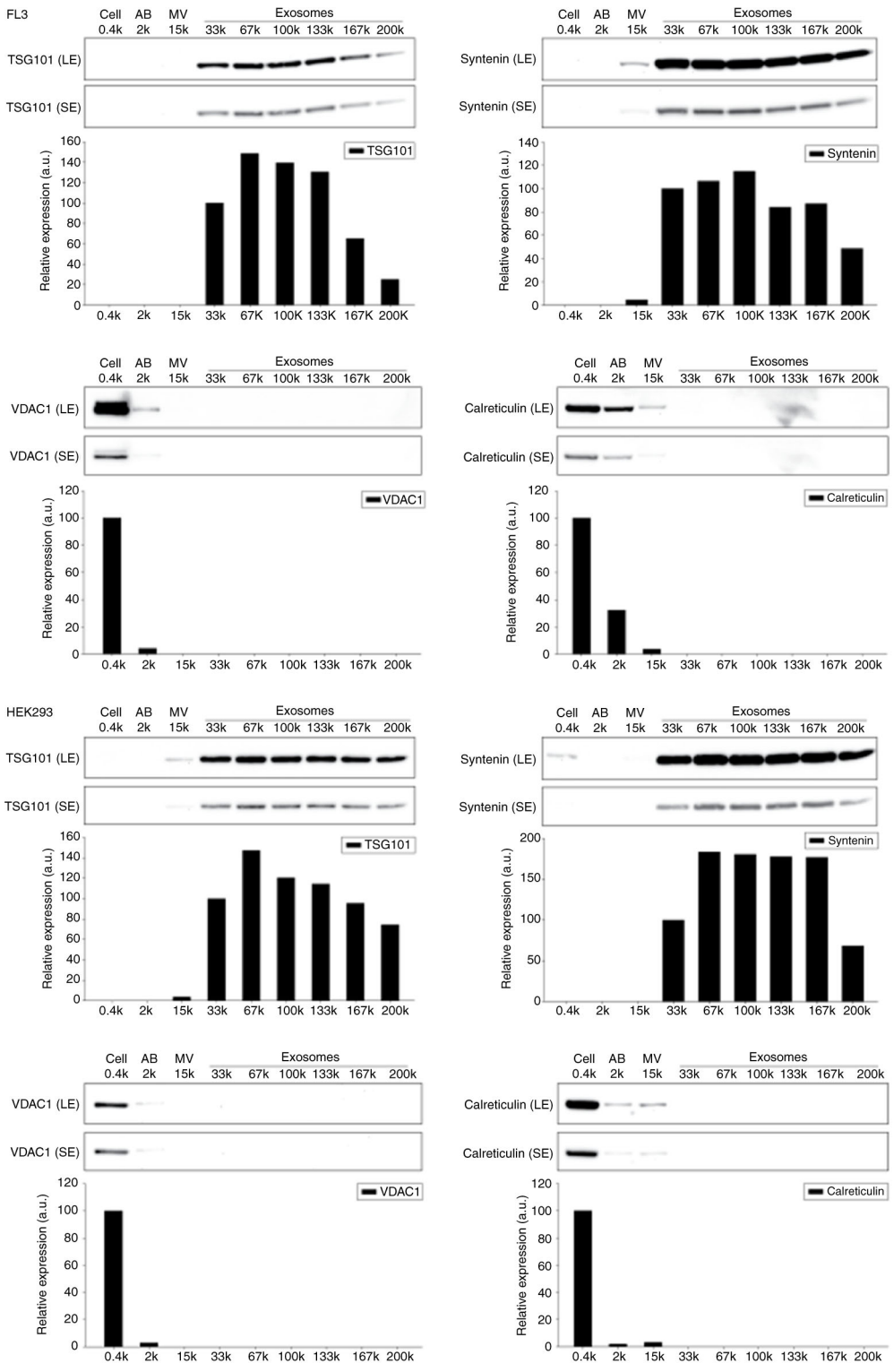

Fig. 5. Immunoblot analysis of TSG101, syntenin, calreticulin and VDAC1 expression in sedimentation pellets after centrifugation at speeds from 0.4k to 200k. An equal amount of total protein (10 μg) was loaded in each well of the gel. Membranes were subjected to long exposures (LE) and short exposures (SE), and the relative levels of expression were assessed by densitometry quantification of the SE blots using Image J software. Because equal amounts of total protein were loaded in each lane, the intensity of the TSG101 and syntenin signals are proportional to the enrichment of exosomal protein in the sample while the intensity of VDAC1 and calreticulin are proportional to the purity of the samples in regard to mitochondrial and ER/microsome contamination, respectively. AB, apoptotic bleb; MV, microvesicle; a.u., arbitrary units.

Citation: Journal of Extracellular Vesicles 2014, **3**: 25011 - http://dx.doi.org/10.3402/jev.v3.25011

the pelleted protein, the predominant fraction of HEK293 extracellular protein was sedimented at 33k rather than from any subsequent spins. For FL3, a gradual pelleting of extracellular protein through g-forces of 33–167k was observed (Fig. 6c). There was a significant linear correlation between the observed depletion of particles and protein for both FL3 (Pearson's $r = 0.85$, $p = 0.034$) and HEK293 (Pearson's $r = 0.85$, $p = 0.030$) through the serial ultracentrifugation steps (Supplementary Fig. 5). The highest ratio of particles-to-protein was achieved at the 67k step for HEK293 while at 100k for FL3 (Fig. 6d). In conclusion, both particle and protein quantification indicated significantly greater sedimentation of extracellular material at lower speeds from HEK293 cells compared to FL3 cells.

To gain insight into the EVs that were pelleted after serial depletions of CCM by ultracentrifugation, we performed immunoblotting for the transmembrane tetraspanin CD81 (10,33), which we previously have found to be highly enriched in exosomes compared to parental FL3 cells (31), as well as TSG101 and syntenin (Fig. 7). Strikingly, for both FL3 and HEK293 cells, there were very strong CD81, TSG101 and syntenin immunoblot signals from pelleted material already at 33k indicating that EVs with exosomal markers could be efficiently isolated at significantly lower speed than the commonly used g-force of 100k or higher. FL3 exosomes were still pelleted at the 100k step while almost all HEK293 exosomes were sedimented already at 67k. CD81 and syntenin signals persisted at higher speeds than the signal from TSG101 for both FL3 and HEK293 exosomes. Normalization of the exosome marker signals revealed that the ratio of signal/protein increased with higher speeds, indicating that exosomal proteins comprised a higher fraction of the total protein in these fractions. The ER/microsome marker calreticulin was efficiently sedimented at 33k and barely present after 67k for FL3, while for HEK293 a substantial amount of calreticulin could still be pelleted at this speed (Fig. 7). In conclusion, EVs bearing exosomal marker proteins could be pelleted to a significant degree already at 33k, a speed which also largely removed remaining microsomal contamination.

Discussion

Exosomes, and other EVs, are present in human biofluids and, thus, may have potential as sources for prognostic and diagnostic disease biomarkers. Exosome research has mostly focused on areas such as their involvement in the tumour microenvironment (34–36) and on their potential as vehicles of drug delivery to therapeutic targets (37,38). However, both the basic investigation of exosomes as well as research into their therapeutic potential requires efficient isolation methods. Purification by ultracentrifugation is the most widely adopted of the basic isolation methods due to its ease and high capacity. In this study, we have examined the impact of ultracentrifugation g-force on the isolation outcome in 2 different cell types.

Surprisingly, a large difference in the sedimentation dynamics of particles and protein in the CCM harvested from FL3 cells compared to HEK293 cells was observed. Consistently, and both when measured as the number of particles and the amount of protein pelleted, HEK293 displayed much more efficient sedimentation of material at lower speeds than FL3. EVs from HEK293 cells bearing the exosomal markers CD81, TSG101 and syntenin could be pelleted already after 90 min at the relatively low g-force of $33{,}000 \times g$, though $67{,}000 \times g$ was more efficient. Material from the CCM of FL3 cells was significantly more resistant to sedimentation though FL3 exosomes could also be pelleted already at $33{,}000 \times g$. The size of particles in the input supernatant from HEK293 cells ($\sim$140 nm) was considerably larger than for FL3 cells ($\sim$100 nm). This may have contributed to the observed differences in sedimentation characteristics (Figs. 4 and 6). Aggregates of proteins can share sedimentation and other biophysical properties with EVs (39). It has been hypothesized that purer EV samples have higher ratios of particles (mainly vesicles) to proteins (vesicle protein and contaminating soluble proteins) and, thus, that such a ratio can be used as a measure of EV sample purity (29). Using this measure, we found that the highest ratio of particles to protein, and thus the purest samples of exosomes, is found after ultracentrifugation at $67{,}000 \times g$ for HEK293 and for $100{,}000 \times g$ for FL3 exosomes (Figs. 4e and 6d). For HEK293 exosomes the highest signal for both exosomal markers TSG101 and syntenin was found after $67{,}000 \times g$. For FL3 exosomes the syntenin signal was highest at $100{,}000 \times g$ and the TSG101 signal slightly higher at $67{,}000 \times g$ (Fig. 4). However, it is worth noticing that it is not clear to what degree particles can be assumed to be vesicles, and not, for example, larger protein aggregates. Especially in light of our finding that considerable amounts of measurable particles remain in samples after overnight ultracentrifugation at $200{,}000 \times g$ (Fig. 2a). With rising centrifugal g-force, we found a continuously increasing quantity of protein in sedimented pellets while there was a tendency for the number of particles counted by NTA to plateau (compare Fig. 4a and d). A possible explanation for this observation is that relatively more protein aggregates or complexes are pelleted at the higher g-forces but due to their small size fall below the detection limit of the NTA technology.

Interestingly, we observed different expression patterns for the 2 exosomal markers TSG101 and syntenin with a marked tendency for a higher syntenin signal from the higher g-force fractions (Fig. 5, parallel experiment) and to persist in these higher speed fractions after depletion (Fig. 7, serial experiment). This could indicate either that

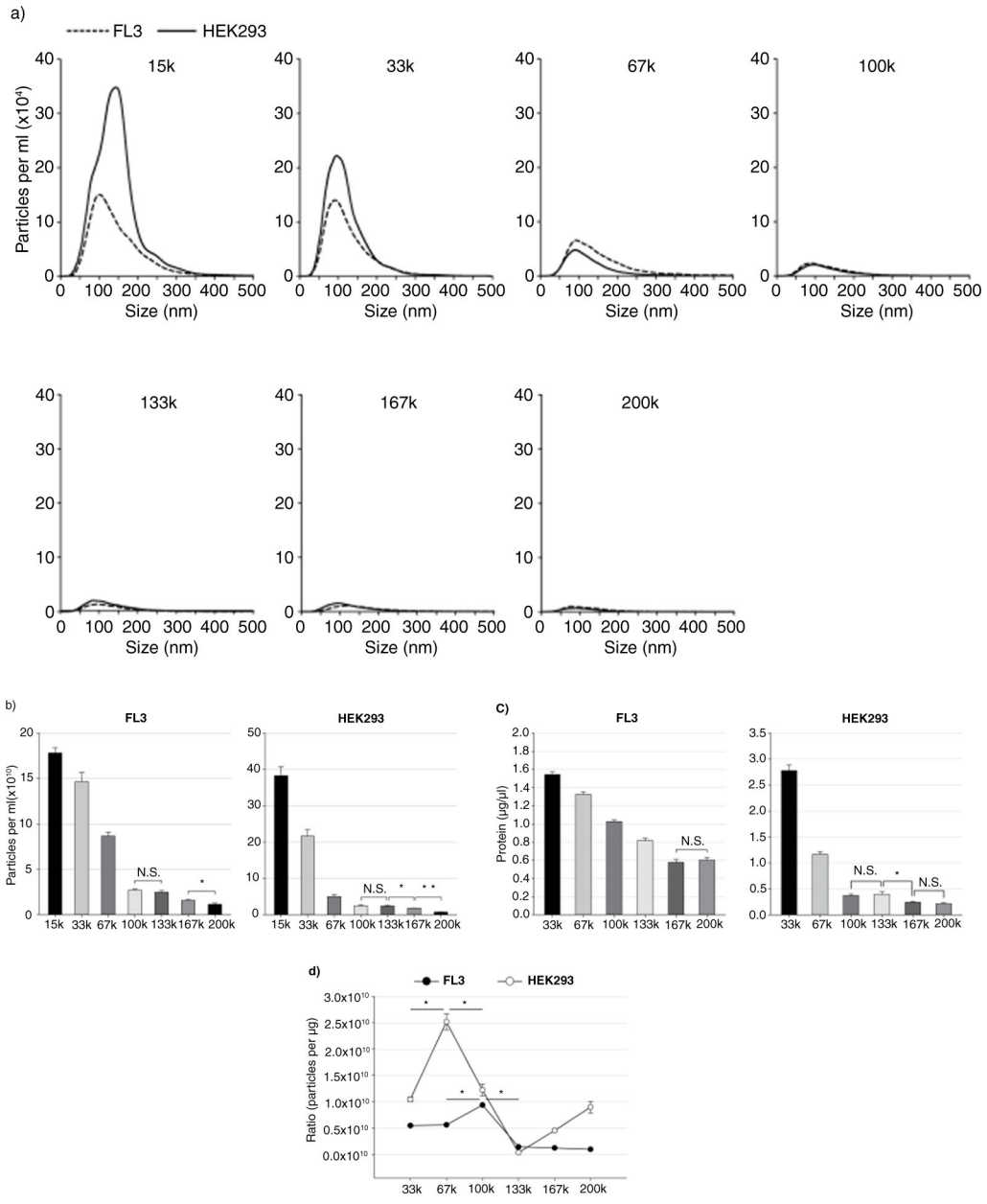

Fig. 6. Serial differential ultracentrifugation. (a) Pre-cleared FL3 and HEK293 CCM supernatants (15k) and supernatants generated by a series of 33–200k ultracentrifugation steps (Table 1) were diluted in particle-free PBS and the particles present measured using the NanoSight NTA system. Data from 2 separate experiments with 5 repeat measurements each for both cell lines was used to generate average plots of the overall size distribution of particles. (b) Quantification by NTA of particles present in supernatants generated from CCM harvested from FL3 (*left*) and HEK293 (*right*) cells and subjected to serial centrifugation steps. Data are expressed as mean $\pm$ s.e.m. ($n = 10$ per group), p-value for overall difference between groups was determined by repeated measures ANOVA (Greenhouse–Geisser corrected) and p-values between pairs of groups were determined by Student's paired t-tests with correction for multiple comparisons by the Holm–Bonferroni procedure. *$p < 0.05$; **$p < 0.0001$; N.S., not significant. (c) Quantification of protein in sedimentation pellets generated by serial centrifugation steps and solubilization in equal volumes of lysis buffer. Data are expressed as mean $\pm$ s.e.m. ($n = 12$ per group), p-value for overall difference between groups was determined by repeated measures ANOVA (Greenhouse–Geisser corrected) and p-values between pairs of groups were determined by Student's paired t-tests with correction for multiple comparisons by the Holm–Bonferroni procedure. *$p < 0.05$; N.S., not significant. (d) The number of pelleted particles was calculated from the input and output supernatants, and the ratio of particles per µg of protein pelleted after serial depletion of pre-cleared FL3 and HEK293 CCM by ultracentrifugation (33–200k) was plotted. Data are expressed as mean $\pm$ s.e.m. ($n = 6$ per group), p-value for overall difference between groups was determined by repeated measures ANOVA (Greenhouse–Geisser corrected) and p-values between pairs of groups were determined by Student's paired t-tests with correction for multiple comparisons by the Holm–Bonferroni procedure. *$p < 0.05$. Reported statistical significance is relative to the maxima (67k for HEK293 and 100k for FL3).

Citation: Journal of Extracellular Vesicles 2014, **3**: 25011 - http://dx.doi.org/10.3402/jev.v3.25011

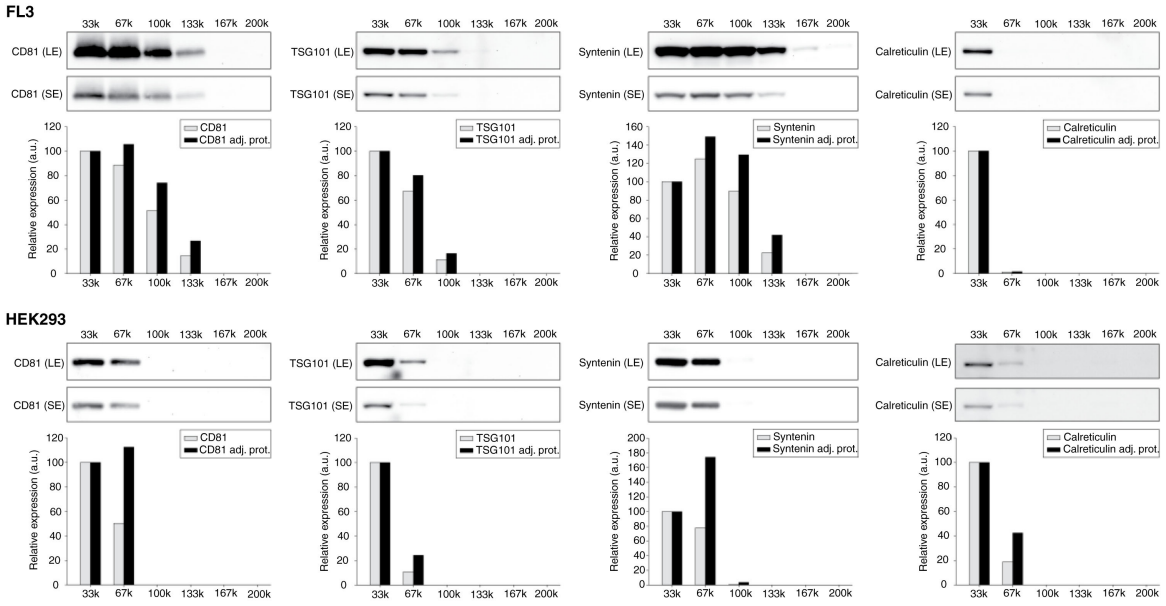

Fig. 7. Immunoblot analysis of CD81, TSG101, syntenin and calreticulin expression after ultracentrifugation of serially depleted CCM. Equal volumes of sample was loaded in each lane corresponding to equivalent fractions of the total samples. Membranes were subjected to long exposures (LE) and short exposures (SE), and the relative levels of expression were assessed by densitometry quantification of the SE blots using Image J software with or without normalization to the quantity of protein in each lane. The relative levels of expression for the 33k centrifugation step were set as 100. Note that for syntenin the LE reveals the presence of the protein after the 167k and 200k steps but complete saturation of the bands for the lower speed centrifugation steps prevents accurate densitometry. a.u., arbitrary units.

syntenin is relatively more highly expressed on smaller and/or less dense exosomes that sediment more efficiently at higher g-forces, while TSG101 is more highly expressed on larger and/or more dense exosomes, or alternatively, that there are sub-populations of exosomes expressing different markers but with overlapping sedimentation profiles.

A major issue in the preparation of pure exosomal isolates from cell culture medium is the contamination that results from cells undergoing apoptosis. While contamination of samples with apoptotic debris can be minimized by using only cultures of cells with a high ($>95\%$) viability, a small degree of dead or dying cells cannot be avoided entirely. Among the possible contaminants are mitochondria but our results indicate that centrifugation at relatively low speed was sufficient to ensure the removal of VDAC1 from CCM of both out tested cell lines (Fig. 5), which is consistent with our previous observations (31). Contamination from the ER compartment, for example in the form of microsomes, is a potential problem in exosome purification. Blotting for the ER-resident proteins calnexin or calreticulin has previously been used to assess ER contamination of exosomal preparations (21,31,40). We did not observe calreticulin in samples that had been pre-cleared up to and including 15k centrifugation and containing a total of 10 μg of protein (Fig. 5, samples 33–200k). We did, however, detect calreticulin in some of our samples pelleted at $33{,}000 \times g$ (Fig. 7) when larger quantities of samples were loaded on the gel. This indicates that contamination from the ER compartment can persist after pre-clearing samples at $15{,}000 \times g$, and is consistent with the presence of calreticulin in microsomes. Based on our results it seems that it is possible to eliminate most of the contamination by inclusion of an additional preliminary $33{,}000 \times g$ step before subsequent isolation of exosomes by higher ultracentrifugation speeds. However, increasing the purity of samples in this manner will also reduce the yield as we have demonstrated, based on the protein markers CD81, TSG101 and syntenin, that exosomes are pelleted already at $33{,}000 \times g$. It should be noted that it is not yet clear from the literature if these protein markers are exclusive to exosomes and not present on other types of EVs such as microvesicles. Previous studies have suggested presence of sub-populations of exosomes expressing different marker proteins (30,41).

Our NTA results for both the FL3 and HEK293 cell lines may indicate that vesicle aggregation occurs as a result of ultracentrifugation. The mode (peak) size of the particles measured in resuspended vesicle sedimentation pellets was in the order of 25 nm larger than particles measured in FL3 CCM supernatant before and after 100k ultracentrifugation (Fig. 1) whilst for HEK293, it was 18 nm (Fig. 4a). The vesicles measured by NTA

directly in suspensions of CCM supernatants are in solution while EVs in pellets are generated by compressing vesicles together on the side/bottom of centrifugation tubes by high centrifugal forces followed by resuspension, typically in PBS (10). Several other investigations that have employed NTA also report modal sizes of exosomes significantly larger than the 40–100 nm size that is generally accepted as the size for this type of EV. Recent examples of sizes for pelleted and resuspended exosomes from different cell lines are 127 nm (MCF7 cells), 117 nm (PC3 cells), 168 nm (MCF10A cells) (42), and 104 nm (mesothelioma cell line) and 109 nm (LNCAP cells) (29). Aggregation of exosomes by ultracentrifugation may, therefore, significantly overestimate the size potentially resulting in unreliable sizing and counting when the pellet of vesicles is resuspended and measured by NTA. We here performed the resuspension of EV pellets in PBS manually by pipetting after ultracentrifugation. More vigorous resuspension of the pelleted exosomes could presumably increase the number of single-exosome particles, but it is unclear how to accomplish this whilst ensuring that exosomes are not damaged and fragmented. It is also possible that exosomes from different cell lines differ significantly in size. In pre-cleared CCM from HEK293 cells, we consistently observed particles $\sim$40 nm larger than the particles in FL3 CCM (Figs. 4a and 6a). In 100,000 $\times g$ pellets, the size difference between HEK293 and FL3 particles was 52 nm (Figs. 1 and 4a). The size of FL3 exosomes as measured by NTA was thus $\sim$86–106 nm, dependent on measurement done on supernatants or resuspended pellets, while for HEK293 the size was $\sim$140–158 nm. This difference could possibly reflect the size of the producing cells as HEK293 cells are significantly larger than FL3 cells.

The relative efficiency of a rotor in pelleting particles is measured by its effective clearing factor (k factor) which is dependent on the RPM with which the rotor is spinning as well as the fill level of the centrifugation tubes. We provide instructions for calculation of the effective k factor for centrifugation of tubes filled to less than nominal capacity and for equalizing runs across different rotor types, in Supplementary File 1. Filling tubes to less than capacity will lead to a shorter average sedimentation path length and thus a reduction in run time compared to tubes filled to nominal capacity (Supplementary Fig. 3). The focus of this study was on the influence of ultracentrifugation g-force. Therefore, the centrifugation time was kept constant at 90 min for all steps in the range of 33,000 $\times g$ to 200,000 $\times g$. Centrifugation force and time are inversely correlated (when the force applied is large enough to overcome the forces opposing movement of the vesicles), thus higher g-forces should require shorter run times and vice versa. We could not, in our limited investigation on a single cell line (FL3 cells, Supplementary Fig. 1), detect a significant increase of protein in pelleted material when the centrifugation time was increased from 90 to 120 min for the Type 70 Ti rotor (100,000 $\times g$, k factor of 158.4). We did, however, see a significant difference in protein yield between 60 and 90 min. It was recently reported that extending the centrifugation time for the Type 70 Ti rotor from 70 to 155 min (118,000 $\times g$, k factor of 133.4) yielded no significant increase in protein yield from conditioned media from the human mast cell line HMC-1, though an increase in RNA yield was observed (43). Sedimentation of material is inevitably influenced to some degree by the centrifugation time but, like we observed for ultracentrifugation g-force, it is likely that the influence of time will vary between cell lines.

As exosome research is a rapidly expanding field there is interest in the development of standard ultracentrifugation isolation protocols in terms of centrifugation g-force and time (9,43). However, we report here that the sedimentation characteristics of exosomes from 2 unrelated cell lines differed significantly. We also found that the 2 cell lines differed in g-force that yielded the optimal ratio of vesicles to total protein, a suggested measure of exosome sample purity. The yield of protein, exosomal or otherwise, obtained by using a specific ultracentrifugation time may also be cell line dependent. These issues highlight the potential difficulties in establishing standard protocols for isolation. While it may be tempting to seek a standardization of protocols in an attempt to minimize discrepancies between reported results from different research group and laboratories, our findings indicate that optimal protocols for exosome purification may well differ between cell lines.

In conclusion, we have conducted a thorough investigation of the influence of ultracentrifugation g-force on the isolation of exosomes. We found that the choice of media impacts the level of background particles, something that may potentially interfere with exosome quantification. We observed marked differences in the fractions obtained by differential centrifugation in terms of vesicle size, protein quantity and relative presence of exosomal markers and contamination markers. These sedimentation profiles showed cell-line-dependent characteristics. Exosomes from both HEK293 and FL3 cells were pelleted at 33,000 $\times g$ but the optimal g-force for sample purity was 67,000 $\times$ g for HEK293 and 100,000 $\times g$ for FL3. Contamination from mitochondria could efficiently be eliminated by low-speed 2,000 $\times g$ centrifugation while ER/microsome contamination could be removed by inclusion of a 33,000 $\times g$ pre-clearing step. The differential expression of the exosome protein markers TSG101 and syntenin in fractions may indicate presence of sub-populations of exosomes preferentially pelleted at different speeds. Taken together, the choice of

Citation: Journal of Extracellular Vesicles 2014, **3**: 25011 - http://dx.doi.org/10.3402/jev.v3.25011

exact g-force, and thus *k* factor, greatly influences exosome purity and yield, and varies across cell lines.

Current research in EVs is challenged by efficient isolation strategies of high specificity that in the same time are practicable. This study suggests that usage of differential centrifugation can be employed to enrich for specific exosome subpopulations. It also stresses that the exact steps of differential centrifugation procedure affects the input for subsequent density gradient centrifugation and therefore should be practiced with awareness. Our main focus here has been the influence of g-force but of equal importance are questions of centrifugation run times. Longer centrifugation run times could conceivably enhance sedimentation of smaller, slower moving subpopulations of exosomes. It would also be of interest to examine the influence of centrifugation run times for obtaining optimal vesicle to total protein ratios. For future studies using differential centrifugation we suggest that the effective *k* factor is reported (or a note is made of the level of tube filling). Finally, we encourage careful consideration and examination of cell-line dependent sedimentation characteristics as differences in sedimentation profiles may impact results profoundly.

Acknowledgements

We thank Maria Engtoft Mark for technical assistance and Prof. Dan Theodorescu (University of Colorado Cancer Center) for providing FL3 cells.

Conflict of interest and funding

This work was supported by grants from The Novo Nordisk Foundation, The Toyota Foundation, Aase and Ejnar Danielsen Foundation, The John and Birthe Meier Foundation, and The Danish Cancer Society. The authors have no conflicts of interest.

References

1. Cocucci E, Racchetti G, Meldolesi J. Shedding microvesicles: artefacts no more. Trends Cell Biol. 2009;19:43–51.
2. Thery C, Ostrowski M, Segura E. Membrane vesicles as conveyors of immune responses. Nat Rev Immunol. 2009;9: 581–93.
3. Simpson RJ, Lim JW, Moritz RL, Mathivanan S. Exosomes: proteomic insights and diagnostic potential. Expert Rev Proteomics. 2009;6:267–83.
4. Vlassov AV, Magdaleno S, Setterquist R, Conrad R. Exosomes: current knowledge of their composition, biological functions, and diagnostic and therapeutic potentials. Biochim Biophys Acta. 2012;1820:940–8.
5. Ostenfeld MS. Cellular disposal of miR23b by RAB27-dependent exosome release is linked to acquisition of metastatic properties. Cancer Res. 2014;74:5758–71.
6. Simons M, Raposo G. Exosomes – vesicular carriers for intercellular communication. Curr Opin Cell Biol. 2009;21: 575–81.
7. Skog J, Wurdinger T, van Rijn S, Meijer DH, Gainche L, Sena-Esteves M, et al. Glioblastoma microvesicles transport RNA and proteins that promote tumour growth and provide diagnostic biomarkers. Nat Cell Biol. 2008;10:1470–6.
8. Lee TH, D'Asti E, Magnus N, Al-Nedawi K, Meehan B, Rak J. Microvesicles as mediators of intercellular communication in cancer – the emerging science of cellular 'debris'. Semin Immunopathol. 2011;33:455–67.
9. Witwer KW, Buzas EI, Bemis LT, Bora A, Lasser C, Lotvall J, et al. Standardization of sample collection, isolation and analysis methods in extracellular vesicle research. J Extracell Vesicles. 2013;2:20360, doi: http://dx.doi.org/10.3402/jev.v2i0.20360
10. Thery C, Amigorena S, Raposo G, Clayton A. Isolation and characterization of exosomes from cell culture supernatants and biological fluids. Curr Protoc Cell Biol. 2006;Chapter 3:Unit 3.22.
11. Raposo G, Stoorvogel W. Extracellular vesicles: exosomes, microvesicles, and friends. J Cell Biol. 2013;200:373–83.
12. Abas L, Luschnig C. Maximum yields of microsomal-type membranes from small amounts of plant material without requiring ultracentrifugation. Anal Biochem. 2010;401: 217–27.
13. Lavoie C, Lanoix J, Kan FW, Paiement J. Cell-free assembly of rough and smooth endoplasmic reticulum. J Cell Sci. 1996;109: 1415–25.
14. Dragovic RA, Gardiner C, Brooks AS, Tannetta DS, Ferguson DJ, Hole P, et al. Sizing and phenotyping of cellular vesicles using Nanoparticle Tracking Analysis. Nanomedicine. 2011;7: 780–8.
15. Gercel-Taylor C, Atay S, Tullis RH, Kesimer M, Taylor DD. Nanoparticle analysis of circulating cell-derived vesicles in ovarian cancer patients. Anal Biochem. 2012;428:44–53.
16. Gardiner C, Ferreira YJ, Dragovic RA, Redman CW, Sargent IL. Extracellular vesicle sizing and enumeration by nanoparticle tracking analysis. J Extracell Vesicles. 2013;2:19671, doi: http://dx.doi.org/10.3402/jev.v2i0.19671
17. Gould SJ, Raposo G. As we wait: coping with an imperfect nomenclature for extracellular vesicles. J Extracell Vesicles. 2013;2:20389, doi: http://dx.doi.org/10.3402/jev.v2i0.20389
18. Lamparski HG, Metha-Damani A, Yao JY, Patel S, Hsu DH, Ruegg C, et al. Production and characterization of clinical grade exosomes derived from dendritic cells. J Immunol Methods. 2002;270:211–26.
19. Keller S, Ridinger J, Rupp AK, Janssen JW, Altevogt P. Body fluid derived exosomes as a novel template for clinical diagnostics. J Transl Med. 2011;9:86.
20. Nolte-'t Hoen EN, van der Vlist EJ, Aalberts M, Mertens HC, Bosch BJ, Bartelink W, et al. Quantitative and qualitative flow cytometric analysis of nanosized cell-derived membrane vesicles. Nanomedicine. 2012;8:712–20.
21. Baietti MF, Zhang Z, Mortier E, Melchior A, Degeest G, Geeraerts A, et al. Syndecan-syntenin-ALIX regulates the biogenesis of exosomes. Nat Cell Biol. 2012;14:677–85.
22. Cantin R, Diou J, Belanger D, Tremblay AM, Gilbert C. Discrimination between exosomes and HIV-1: purification of both vesicles from cell-free supernatants. J Immunol Methods. 2008;338:21–30.
23. Yuana Y, Levels J, Grootemaat A, Sturk A, Nieuwland R. Co-isolation of extracellular vesicles and high-density lipoproteins using density gradient ultracentrifugation. J Extracell Vesicles. 2014;3:23262, doi: http://dx.doi.org/10.3402/jev.v3.23262
24. Mitchell JP, Court J, Mason MD, Tabi Z, Clayton A. Increased exosome production from tumour cell cultures using the Integra CELLine Culture System. J Immunol Methods. 2008;335:98–105.
25. Ostenfeld MS, Bramsen JB, Lamy P, Villadsen SB, Fristrup N, Sorensen KD, et al. miR-145 induces caspase-dependent

and -independent cell death in urothelial cancer cell lines with targeting of an expression signature present in Ta bladder tumors. Oncogene. 2010;29:1073–84.
26. Nicholson BE, Frierson HF, Conaway MR, Seraj JM, Harding MA, Hampton GM, et al. Profiling the evolution of human metastatic bladder cancer. Cancer Res. 2004;64:7813–21.
27. Quah BJ, O'Neill HC. Mycoplasma contaminants present in exosome preparations induce polyclonal B cell responses. J Leukoc Biol. 2007;82:1070–82.
28. Yang C, Chalasani G, Ng YH, Robbins PD. Exosomes released from Mycoplasma infected tumor cells activate inhibitory B cells. PLoS One. 2012;7:e36138.
29. Webber J, Clayton A. How pure are your vesicles? J Extracell Vesicles. 2013;2:19861, doi: http://dx.doi.org/10.3402/jev.v2i0.19861
30. Bobrie A, Colombo M, Krumeich S, Raposo G, Thery C. Diverse subpopulations of vesicles secreted by different intracellular mechanisms are present in exosome preparations obtained by differential ultracentrifugation. J Extracell Vesicles. 2012;1:18397, doi: http://dx.doi.org/10.3402/jev.v1i0.18397
31. Jeppesen DK, Nawrocki A, Jensen SG, Thorsen K, Whitehead B, Howard KA, et al. Quantitative proteomics of fractionated membrane and lumen exosome proteins from isogenic metastatic and nonmetastatic bladder cancer cells reveal differential expression of EMT factors. Proteomics. 2014;14:699–712.
32. Khatua AK, Taylor HE, Hildreth JE, Popik W. Exosomes packaging APOBEC3G confer human immunodeficiency virus resistance to recipient cells. J Virol. 2009;83:512–21.
33. Perez-Hernandez D, Gutierrez-Vazquez C, Jorge I, Lopez-Martin S, Ursa A, Sanchez-Madrid F, et al. The intracellular interactome of tetraspanin-enriched microdomains reveals their function as sorting machineries toward exosomes. J Biol Chem. 2013;288:11649–61.
34. Bobrie A, Thery C. Exosomes and communication between tumours and the immune system: are all exosomes equal? Biochem Soc Trans. 2013;41:263–7.
35. Camussi G, Deregibus MC, Tetta C. Tumor-derived microvesicles and the cancer microenvironment. Curr Mol Med. 2013;13:58–67.
36. Kucharzewska P, Belting M. Emerging roles of extracellular vesicles in the adaptive response of tumour cells to microenvironmental stress. J Extracell Vesicles. 2013;2:20304, doi: http://dx.doi.org/10.3402/jev.v2i0.20304
37. Kosaka N, Takeshita F, Yoshioka Y, Hagiwara K, Katsuda T, Ono M, et al. Exosomal tumor-suppressive microRNAs as novel cancer therapy: "exocure" is another choice for cancer treatment. Adv Drug Deliv Rev. 2013;65:376–82.
38. EL Andaloussi S, Mager I, Breakefield XO, Wood MJ. Extracellular vesicles: biology and emerging therapeutic opportunities. Nat Reviews Drug Dis. 2013;12:347–57.
39. Gyorgy B, Modos K, Pallinger E, Paloczi K, Pasztoi M, Misjak P, et al. Detection and isolation of cell-derived microparticles are compromised by protein complexes resulting from shared biophysical parameters. Blood. 2011;117:e39–48.
40. Saunderson SC, Schuberth PC, Dunn AC, Miller L, Hock BD, MacKay PA, et al. Induction of exosome release in primary B cells stimulated via CD40 and the IL-4 receptor. J Immunol. 2008;180:8146–52.
41. Colombo M, Moita C, van Niel G, Kowal J, Vigneron J, Benaroch P, et al. Analysis of ESCRT functions in exosome biogenesis, composition and secretion highlights the heterogeneity of extracellular vesicles. J Cell Sci. 2013;126:5553–65.
42. Yoshioka Y, Konishi Y, Kosaka N, Katsuda T, Kato T, Ochiya T. Comparative marker analysis of extracellular vesicles in different human cancer types. J Extracell Vesicles. 2013;2:20424, doi: http://dx.doi.org/10.3402/jev.v2i0.20424
43. Cvjetkovic A, Lotvall J, Lasser C. The influence of rotor type and centrifugation time on the yield and purity of extracellular vesicles. J Extracell Vesicles. 2014;3:23111, doi: http://dx.doi.org/10.3402/jev.v3.23111